Brodogradnja/Shipbilding/Open access Volume 73 Number 3, 2022

Milovan Perić

http://dx.doi.org/10.21278/brod73303

ISSN 0007-215X
eISSN 1845-5859

PREDICTION OF CAVITATION ON SHIPS

UDC 532.528: 62-253.6: 621.43.013.6
Original scientific paper

Summary

The emphasis of this paper is on challenges in simulation of cavitating flows, especially flows around propeller and rudder. First the sources of errors in predictions based on Computational Fluid Dynamics (CFD) are highlighted: the accuracy of geometry, grid quality and fineness, turbulence modeling and cavitation modeling. The interaction between errors from different sources is also discussed. The importance of turbulence in the flow upstream of propeller and the difficulty of accounting for it is described next. Special attention is paid to the prediction of tip-vortex cavitation and to scale effects. Results from simulations are compared to experimental data from SVA Potsdam, except for the full-scale analysis of flow around hull, propeller and rudder, for which no experimental data is available. It is concluded that cavitation can be predicted to a degree which makes simulation an indispensable tool for design and optimization of maritime vessels.

Key words: *simulation; flow; propeller; cavitation*

1. Introduction

Cavitation is an important phenomenon which occurs in many flows, including those around propeller and rudder. The main cause is flow acceleration, leading to pressure falling locally below saturation level for given temperature. A typical example of such flow acceleration is the propeller blade; the lowest pressure is usually found on the suction side close to the leading edge. However, flow acceleration can also happen due to wall vibration, especially at high frequencies and/or amplitudes of motion. In most cavitating flows, a relatively small amount of liquid evaporates, compared to the total flow rate. The heat needed for the phase change is taken from the surrounding liquid, but due to the small amount of liquid that evaporates, temperature in liquid is usually assumed to stay constant.

The phase change happens at the interface between liquid and gas phase. A perfectly purified liquid, without any solid particles or bubbles of non-condensable gases, can sustain large tensile stresses (i.e., negative absolute pressure). The lowest measured pressure in water (before cavitation started) known to the author was around –280 bar [1]. However, liquids encountered in engineering and nature are far from being pure; they contain seed bubbles (either bubbles of non-condensable gases like air, or gas inclusions in crevices on solid

particles) from which phase change can start, leading to cavitation bubbles which can grow and collapse. In some flow zones where bubble residence times are relatively long (e.g., in recirculation zones), bubbles can grow so large that they merge and form a vapor sheet or cloud in which the vapor volume fraction can become very large (close to 100%). On the other hand, in regions of high-speed flow cavitation bubbles my quickly cross the low-pressure zone and in spite of high growth rate, the vapor volume fraction can still remain relatively low.

Cavitation not only adversely affects the performance of the flow device – it also leads to vibration, noise and erosion and could even cause structural damage. It is therefore important to be able to predict with an acceptable accuracy whether cavitation takes place at a particular operating point and what kind of cavitation it is, in order to take mitigating measures.

Nowadays computational methods are regularly used to investigate all aspects of fluid flows. Computational fluid dynamics (CFD) plays a major role in the development of new products and their optimization, and is part of a virtual or "digital twin" approach to product development. Complex geometries can be imported directly from CAD-tools, the computational grid is generated automatically and it can be locally refined where higher resolution is required. Most commercial and public CFD-codes are based on finite-volume methods; these methods are described in detail in Ferziger et al [2].

Most engineering flows in which cavitation occurs are turbulent; this is especially true for the flow around ship and propeller at full scale. Because one cannot afford to resolve all turbulent fluctuations in space and time, simulation of such flows by solving directly the Navier-Stokes equations is not possible. When computing the flow around a ship hull (with or without a propeller), one has to use the Reynolds-averaged Navier-Stokes (RANS) equations instead. The effects of turbulence are accounted for by using one of many available turbulence models. The most widely used models are of eddy-viscosity type; they determine the so-called *turbulent viscosity* by solving two additional equations. Turbulent viscosity (which may vary by several orders of magnitude within the solution domain) is then added to the fluid viscosity. Other methods require solution of additional equations for the Reynolds-stress components and the dissipation rate, which are in general stiffer and more difficult to solve. For more details on RANS-based simulation approaches, see books on this subject and references therein [3-6].

When the Reynolds number of the cavitating flow is moderate (e.g. when simulating the flow around propeller in model scale), one can use methods based on large-eddy simulation (LES), in which filtered Navier-Stokes equations are solved. Larger scales from turbulence spectrum are resolved and the smaller scales – which are more universal in nature – are modeled. For this approach, one needs to use finer grids and smaller time steps than in RANS-based methods. The modeling of subgrid-scale turbulence (i.e., the part of turbulence spectrum which cannot be resolved by the computational grid and time steps) is usually achieved using algebraic models, like the one from Smagorinsky [7] or the WALE model [8].

Other features of engineering flows which cannot be fully resolved (like cavitation, interaction of multiple phases etc.) also need to be modeled, meaning that equations solved in CFD are not exact – even their exact solution would not describe the reality correctly. Errors are also introduced through discretization and iterative solution of discretized equations.

The aim of this paper is to highlight the most important aspects of simulation of cavitating flows around ship propellers and rudders, assess the relative impact of potential errors on simulation accuracy and indicate how the errors can be reduced. CFD delivers only *approximate solutions* even for simple flows and the importance of error assessment cannot be overemphasized.

Iteration errors (due to the fact that the discretized governing equations are solved iteratively and iterations have to be stopped at some stage) are relatively easy to control by monitoring the residuals and quantities of particular interest (like thrust and torque on a propeller). When residuals are reduced by say 4 orders of magnitude, one can expect that variable values are not changing on three to four most significant digits, which is usually enough; that corresponds to iteration errors being on the order of 0.1% or smaller. Different convergence criteria are applied when solving the linearized equation systems, to non-linear iterations in transient problems and in steady-state computations; for more details, see [2].

Discretization errors depend on the choice of approximations used in different discretization steps (approximation of surface, volume and time integrals; interpolation of variables to locations other than the computational point; approximation of gradients etc.), and on the properties of the computational grid. For given selections, discretization errors can only be reduced by systematically refining the grid, i.e. by reducing the grid spacing. However, the comparison of results from a series of systematically refined grids may be deceiving if the original grid design is unsuitable to resolve all the relevant flow features. This will be examined in Sect. 7.

Modeling errors are usually the largest and most difficult to estimate when simulating cavitating flows. There are many possible sources of such errors, the major ones being:

- Turbulence model (cf. Sect. 5);
- Cavitation model (cf. Sect. 2);
- Geometry of the solution domain not being the same as in reality (cf. Sect. 4);
- Boundary conditions not corresponding to reality;
- The use of two-dimensional approximation (cf. Sect. 3), incorrect fluid properties, etc.

What makes the assessment of accuracy of numerical simulations difficult is the fact that errors from different sources interact with each other: they may partially cancel out or augment each other, depending on their sign and magnitude. In order to minimize such effects, it is important to ensure that iteration errors are at least an order of magnitude lower than discretization errors, and that discretization errors are at least an order of magnitude lower than modeling errors.

Simulation of cavitating flow around propellers and hydrofoils is the subject of regular symposia (Symposium on Marine Propulsors [9], International Symposium on Cavitation, Symposium on Naval Hydrodynamics); in proceedings of these symposia, many useful information about application of CFD to cavitating flows can be found. The results presented in this paper were obtained by the author using the *Simcenter STAR-CCM+* software and both discretization methods and physics models which are available in most commercial and public CFD software and are widely used in engineering practice. Most of these simulations were specifically conducted to highlight the main topics of the paper.

In the following section the most widely used cavitation models are briefly described, followed by a discussion of suitability of two-dimensional approximations for the simulation of cavitating flows. Next, the accuracy of the flow domain geometry representation in simulation is discussed. This is followed by a section devoted to the effects of turbulence modeling approach. Section 6 is devoted to incipient cavitation and Section 7 to the prediction of tip-vortex cavitation. In Section 8 the scale effects are discussed, followed by concluding remarks.

2. The Most Widely Used Cavitation Models

Most cavitation models are based on the assumption that liquid contains seeds from which cavitation bubbles can grow when the pressure becomes lower than saturation pressure. The number of seeds per cubic meter of liquid and their initial diameters are parameters of the model, by which the purity or treatment of the liquid (like filtering or degassing) can be taken into account. The modeling is usually based on the homogeneous two-phase flow assumption: equations of motion are solved for a single effective fluid, and the distribution of vapor and liquid phase is determined by solving an additional equation for the vapor volume fraction. This is similar to the Volume-of-Fluid (VOF) method for the prediction of free-surface flows, with two distinctions:

- The equation for vapor volume fraction contains a source term, which governs the phase change (i.e., the growth and collapse of cavitation bubbles) and leads to a non-zero divergence of the velocity field.
- Because vapor volume fraction in a cavitating flow can vary smoothly between 0 and 1, a sharp interface between the phases may in general (on the macroscopic scale) not be present. Therefore, the special interface-capturing schemes for convection fluxes aimed at producing a sharp interface in free-surface flows are not used; instead, the schemes used for convection fluxes in momentum or scalar transport equations are used.

The source term is based on an estimate of bubble growth or collapse rate, which is usually based on the Rayleigh-Plesset or a similar equation. The widely used version of the Rayleigh-Plesset equation reads:

$$R\frac{\mathrm{d}^2R}{\mathrm{d}t^2}+\frac{3}{2}\left(\frac{\mathrm{d}R}{\mathrm{d}t}\right)^2=\frac{p_s-p}{\rho_1}-\frac{2\sigma}{\rho_1 R}-4\frac{\mu_1}{\rho_1 R}\frac{\mathrm{d}R}{\mathrm{d}t} \tag{1}$$

In this equation, R stands for bubble radius, t is time, p_s is the saturation pressure for given temperature, p is the pressure in liquid surrounding the bubble, ρ_l is liquid density, σ is the surface tension coefficient for given temperature, and μ_l is the dynamic viscosity of liquid.

Computing the bubble growth rate $\mathrm{d}R/\mathrm{d}t$ from this equation is not trivial; however, because the Navier-Stokes equations are solved iteratively within each time step, one can devise an iteration procedure for the computation of $\mathrm{d}R/\mathrm{d}t$ from the above equation. A model based on this approach was used in [10] and it produced good results. However, due to the complexity of the equation, the problem is stiff and small time steps or strong under-relaxation are required, which is why simpler methods are usually preferred.

The most widely used cavitation model in commercial and public CFD-codes is the Schnerr-Sauer model [11], in which the bubble growth rate is determined from a simplified expression containing only the terms next to equal sign on each side of the above equation. This quadratic equation cannot be solved when the pressure in the liquid surrounding a bubble is higher than the saturation pressure, because $(p_s - p)$ is then negative. The problem is solved by using the absolute value of this pressure difference and, if it was negative, adding a minus sign to the result. This is mathematically not correct; however, as a semi-plausible approximation, this has proven to still lead to acceptable solutions:

$$\frac{\mathrm{d}R}{\mathrm{d}t}=\mathrm{sign}\left(p_s-p\right)\sqrt{\frac{2}{3}\frac{|p_s-p|}{\rho_1}} \tag{2}$$

The Schnerr-Sauer model is very robust and in most engineering applications leads to solutions of acceptable accuracy, as will be shown in the following sections. It is the most widely used model in engineering and is available in all major commercial and public CFD-codes. Because of the above-mentioned crude approximation, the model has often been blamed for errors which came from other sources; an example will be shown in Sect. 7.

Several other cavitation models based on a similar approach as that used in the Schnerr-Sauer model are available in commercial and public CFD-codes; they usually differ in coefficients multiplying the bubble growth rate in the source term of volume fraction equation (often taken to be different for growth and collapse). Another class of cavitation models are the so-called barotropic models, which are based on a special equation of state which turns liquid into vapor instantly when pressure falls below saturation level and vice-versa. These models do not use the bubble seed density and initial diameter as parameters, which is sometimes advertised as an advantage relative to models based on bubble dynamics. As a consequence, they cannot account for the effects of liquid treatment (filtration, degassing), which are known to significantly affect the cavitation process and may even suppress the cavitation completely. Neither the numerical methods nor cavitation models will be discussed in any more detail here, because the focus of this paper is on other aspects of simulation of cavitating flows and the findings are applicable to any method or model.

3. Two-Dimensional Approximation

When the geometry is axi-symmetric or does not change in the spanwise direction, a two-dimensional (2D) approximation is often used to reduce the computational effort. This is usually justifiable for single-phase, statistically steady flows. However, cavitating flows are often strongly unsteady and almost always three-dimensional. An example is cloud cavitation on propellers and rudders, which is characterized by periodic growth and detachment of the vapor cloud made of many bubbles of various sizes. Unsteady flows are anyway usually strongly three-dimensional (3D); by constraining the velocity field to two dimensions in a 2D-simulation, many features of cavitating flows observed in experiments cannot be adequately simulated.

Figure 1 shows representative pictures from 2D and 3D simulations based on Reynolds-averaged Navier-Stokes (RANS) equations and from one large-eddy (LES) simulation, performed using the Schnerr-Sauer cavitation model [11], for the flow around a NACA0015 hydrofoil at 10.3° angle of attack. The chord length of the foil was 0.2 m, flow speed was 6 m/s, the absolute pressure in the cavitation tunnel was 32,900 Pa and the saturation pressure for water at given temperature was 2,300 Pa (cavitation number 1.7). In a 2D-simulation, the build-up of a large cavitation zone and its detachment are obtained, but the features of the flow are substantially different from those observed in experiment. A 3D simulation based on the RANS-approach and using the k-ε turbulence model produces a significant improvement in solution quality. However, only a LES-type analysis leads to solutions which exhibit similar flow features as seen in experiment, even when a simple cavitation model (Schnerr-Sauer [11]) is used, as can be clearly seen by comparing the three numerical solutions with an experiment performed at HSVA Hamburg (unpublished data). The reason is that the nature of LES for the simulation of turbulence (transient computation using finer grids and smaller time steps than in RANS-based simulations) captures more of the cavitation bubble dynamics. Similar conclusions regarding comparisons of RANS and LES-type solutions were drawn in [10], where the additional benefit of using a more advanced cavitation model (based on the full Rayleigh-Plesset equation) is also documented. Thus, the modeling errors from 2D

approximation and from RANS approach are more significant than the errors from cavitation modeling.

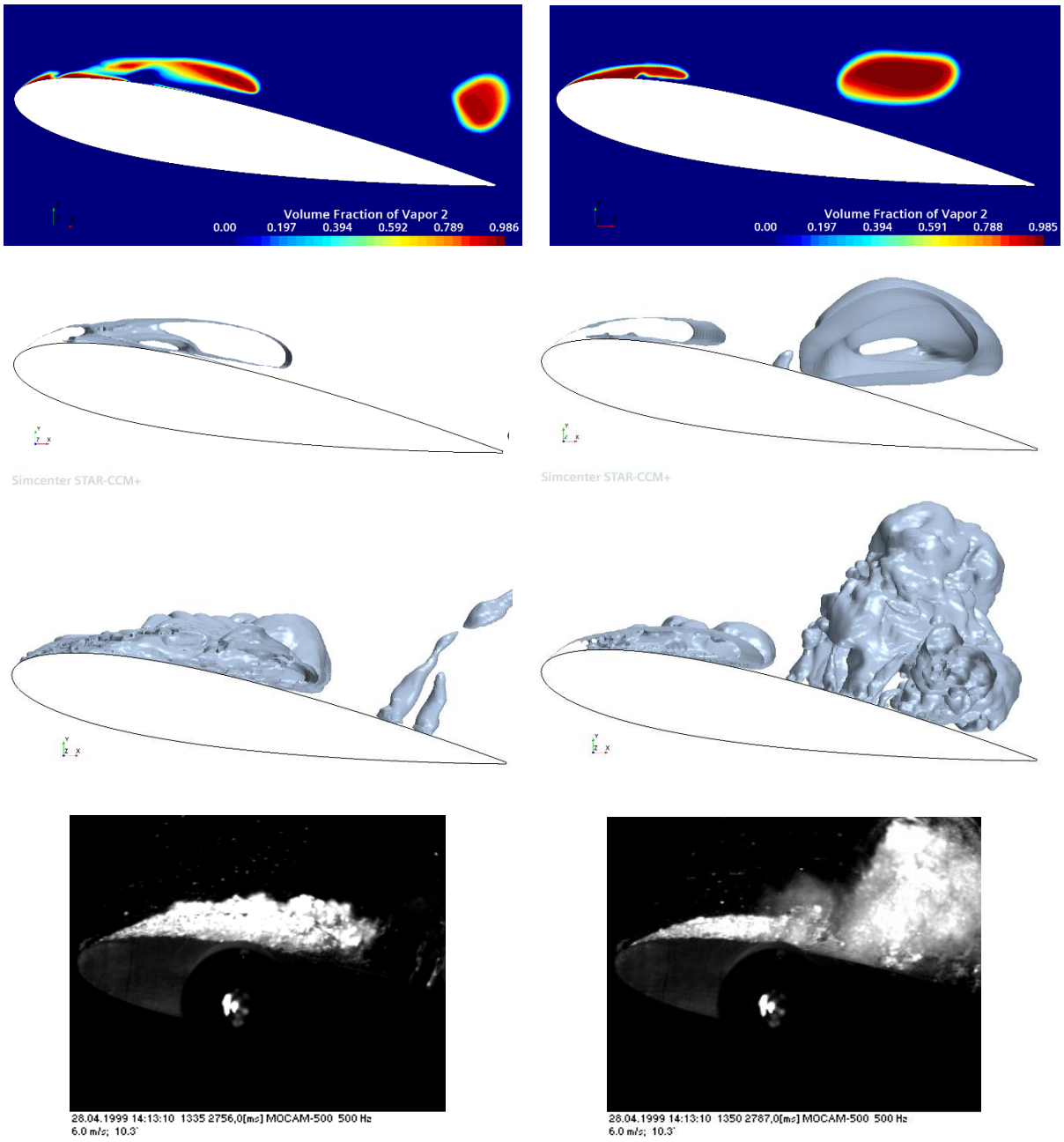

Figure 1 Cavitation on a NACA0015 hydrofoil, spanned between side walls of a cavitation tunnel: distribution of vapor volume fraction in a 2D unsteady RANS simulation (1st row), the side view of iso-surfaces of vapor volume fraction 0.05 from a 3D unsteady RANS simulation (2nd row) and from a LES-simulation (3rd row), and the side view of cavitation bubbles in an experiment (bottom row).

4. Accuracy of Geometry

In numerical simulations of fluid flow, the geometry of the solution domain is taken from a CAD model. In a CAD model of a propeller, all blades are identical and the circumferential distance between them is the same. However, the geometry of a manufactured propeller used in model tests or on the real vessel usually differs from CAD. One reason is the manufacturing tolerance (e.g. the casting process, followed by the manual final surface

preparation and polishing). Model-scale propellers, used for physical testing in towing tanks, typically have a diameter between 0.2 and 0.25 m. This makes it particularly difficult to achieve the blade shape specified in the CAD-model. International Towing Tank Conference (ITTC) specifies in its guidelines that a model-scale propeller for tests should be manufactured with 0.1 mm tolerance (0.05 mm for the leading end trailing edges).

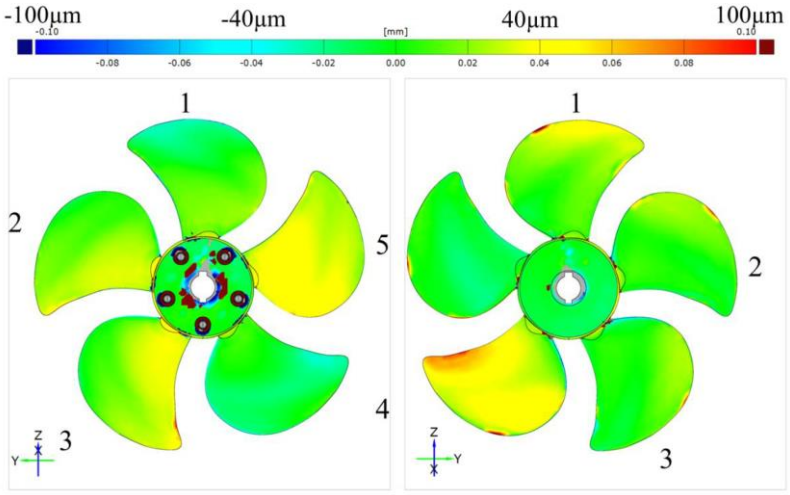

Figure 2 Deviation of the manufactured geometry from CAD model, Potsdam Propeller Test Case [12].

In order to assess the differences between the manufactured propeller and the CAD-model, SVA Potsdam [12] performed detailed measurements of the built geometry of two samples of their Potsdam Propeller Test Case (PPTC). Figure 2 shows the deviations of suction and pressure side from CAD model for all five blades. While the deviations are clearly within the ITTC recommendation, it is also obvious that each blade is different. For example, blade 5 is almost identical to CAD geometry on suction side, but around 0.05 mm off on pressure side. The same is true for blade 4, where the pressure side is perfect and the suction side is up to 0.1 mm off.

While the optical scanning of suction and pressure side of propeller blades is relatively easy, measuring the shape of leading and trailing edges is very difficult. SVA Potsdam is since 2016 able to make such measurements and performed a detailed assessment of leading edge geometry for two versions of the PPTC-propeller (controllable pitch and fixed pitch) along the contour of constant radius $r = 0.7R$, where R is the outer propeller radius. Figure 3 shows the contours of the two manufactured propellers together with the contour taken from the CAD model. The CAD model geometry exhibits a pronounced „nose“ at the leading edge, with a very small radius of curvature, followed by short sections on both sides which are almost straight lines at the end of which larger radii of curvature connect these lines to the blade contour on pressure and suction sides. Both manufactured profiles have a smoothly varying curvature of the leading edge, which is significantly different from the CAD-shape (although being within the tolerance specified by ITTC). The consequence is that both the stagnation line (along which the flow splits to suction and pressure side streams) and the possible tendency to flow separation and cavitation may be significantly influenced by the difference between the CAD-geometry (which is used to define the flow domain in numerical simulations) and the manufactured blades.

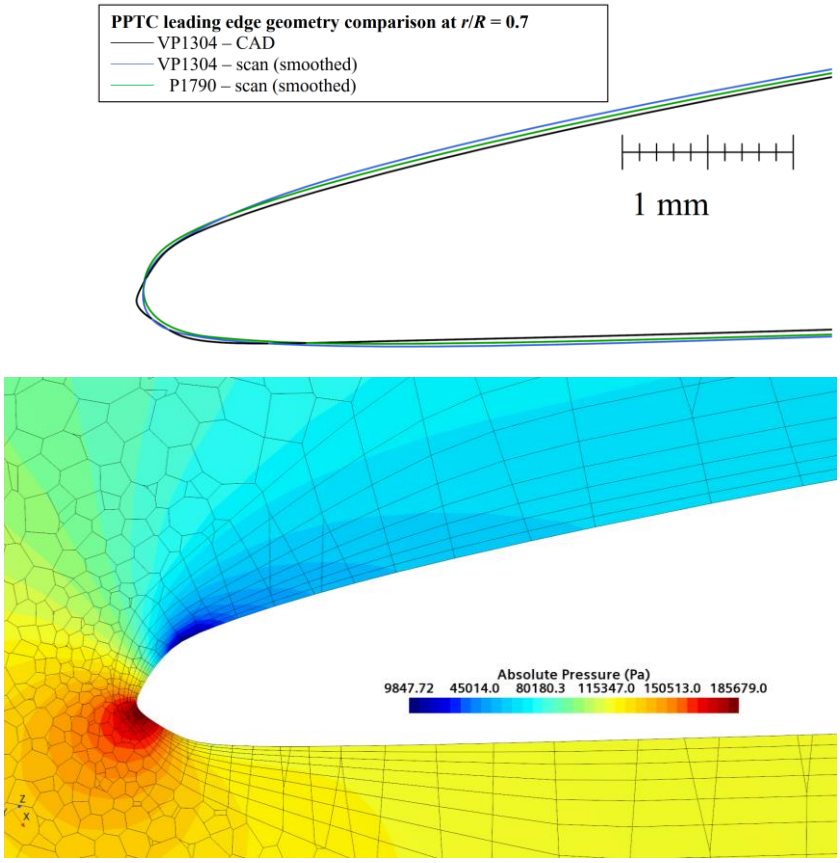

Figure 3 Deviation of the two manufactured blade profiles from CAD at r/R = 0.7 (upper [12]) and the cut through the numerical grid at the same radius with the computed pressure distribution (lower). The scale in the upper plot is 1 mm long with 0.1 mm subdivisions.

Figure 3 also includes a plot of the grid with pressure distribution from a simulation of non-cavitating flow (open-water test) around PPTC. In this simulation the wall functions were used to specify the boundary conditions at walls, but even in that case the thickness of the first cell at wall is of the same order of magnitude as the difference between the manufactured propeller and the CAD model. If the viscous boundary layer near wall is to be resolved by the grid, the first cell next to wall would have had to be more than 10 times thinner (ca. 0.005 mm, compared to ca. 0.05 mm in Fig. 3). This is required when using the low-Re wall treatment in RANS-computations or when using the LES approach to turbulence modeling; see Sect. 5. In that case, several near-wall prism layers in the computational grid would fall within the difference between the CAD-profile and the manufactured profile. Also, the blade is thicker in both manufactured models than in the CAD-model; in the middle of the blade part shown in Fig. 3, the thickness difference is about 9%.

Unfortunately, there is no full CAD-model of the manufactured geometry, which could be used to generate the grid for flow simulation in a domain bounded by the built geometry. Only by comparing solutions obtained using CAD geometry and built geometry would it be possible to reliably assess the significance of the observed discrepancy between the manufactured propellers and the CAD-model. Jin et al. [13] studied the effects of simplified leading-edge defects on the 2D single-phase flow around an airfoil and found that defects within the allowed tolerance can significantly affect cavitation inception. It would also be important to assess the effects of the difference between individual propeller blades, but this too requires a CAD-model of the built geometry. We hope that such data will become available in the near future.

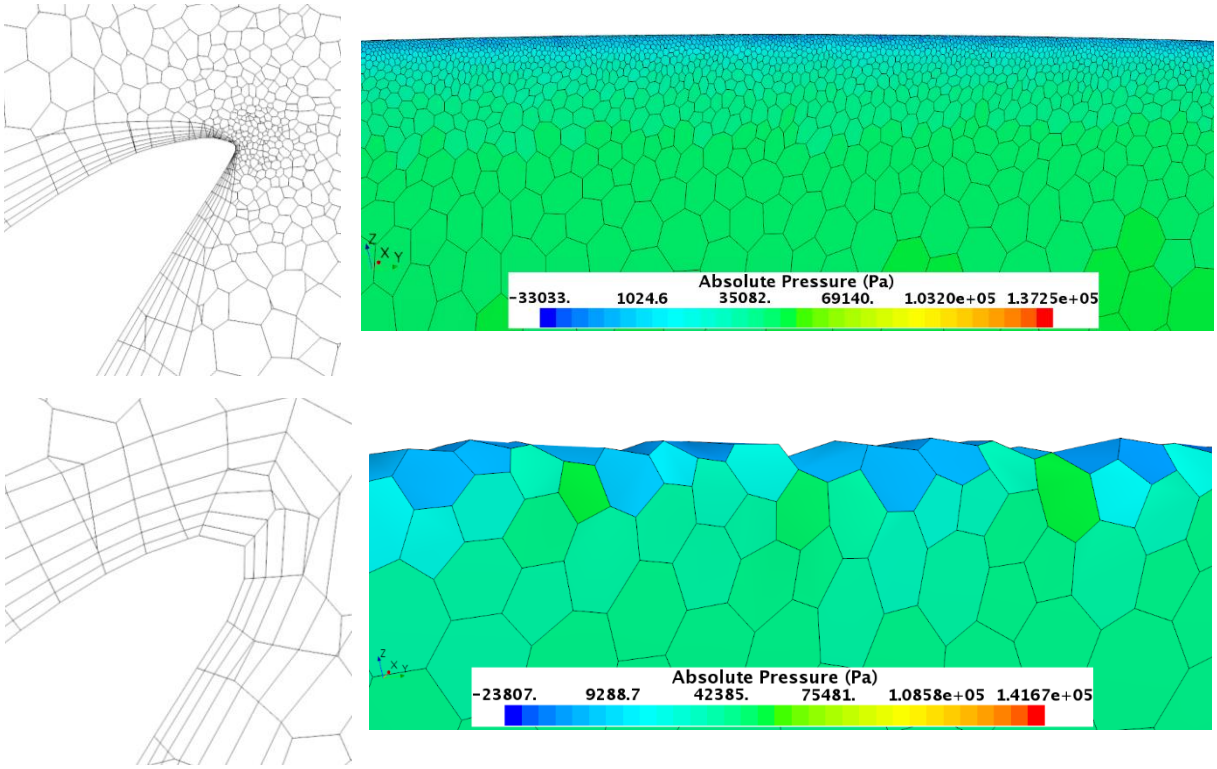

Figure 4 Representation of the leading-edge geometry by the computational grid, in a longitudinal section through propeller blade (left) and in a view onto blade from suction side (right), from a locally refined grid (upper) and from a coarse grid (lower).

Even when the correct geometry of the flow domain is available as input, the generated grid may not produce an accurate representation of it. Especially when the CAD model contains parts with very small curvature radii, it is easy to falsify the geometry if the grid is not locally sufficiently refined. An example is presented in Fig. 4, showing a longitudinal cut through the polyhedral grid around the PPTC-propeller and a surface view of the leading edge for two grids. In one grid the leading-edge zone was locally refined so that the wall curvature is relatively accurately represented (minimum cell size 0.011 mm), while in the other grid no special measures were taken to refine the grid where the wall curvature is high (minimum cell size 0.176 mm); further away from the leading edge, the two grids have cells of a similar size.

As can be seen in Fig. 4, the coarse grid representation of the leading edge geometry is far from the CAD geometry; the curvature is not resolved and the leading edge is very rough. Obviously, the two grids represent two substantially different geometries of propeller blade near leading edge. Thus, when the solutions from these two grids are compared, the difference is not only due to different cell size in critical zones, but also due to different shapes of propeller blade. Simulations were performed with both grids for a single blade with periodic conditions in circumferential direction. The coarse grid had 930,649 cells and the grid with local refinement along leading edge had 3,309,770 cells.

With the view of different leading-edge resolution, one would expect a significant difference in solutions obtained with the two grids depicted in Fig. 4. The blunt and rough form of the leading edge from the coarse grid suggests that the solution should be significantly in error. However, the comparison of thrust and torque computed on the two grids leads to a surprise: the results do not differ much! Table 1 presents the thrust and torque computed on the two grids and the measured values [14].

Table 1 Comparison of results from two grids shown in Fig. 4 with experimental data of SVA Potsdam [14] (numbers in parenthesis represent the difference to experiment).

	Experiment	Coarse grid	Locally refined grid
Thrust	181.74 N	183.4 N (+0.91 %)	182.95 N (+0.67 %)
Torque	11.796 Nm	12.13 Nm (+2.83 %)	12.06 Nm (+2.24 %)

As can be seen from Table 1, the difference between solutions obtained on the two grids is much smaller than the difference between either solution and experimental data. One may ask: how is that possible? The answer lies in partial cancellation of errors. Because of the randomness of the leading edge „roughness“ caused by the too coarse grid, local errors along leading edge vary in amplitude and sign, and when the forces are integrated over the whole blade, positive and negative errors partially cancel out. However, one cannot expect that such partial cancellation will happen for every operating point or for every propeller; it would be foolish to conclude that, because the results agree well with experiment, the coarse grid is “good enough”. Sharp edges resulting from the coarse grid where the curvature of geometry is high can lead to flow separation or cavitation where it should not happen. For reliable solutions – especially when simulating cavitation – one needs to design the grid such that important geometry features are adequately resolved.

5. Accounting for Turbulence

Certain flow phenomena cannot be captured well when a RANS approach is used. An example is the begin of suction-side cavitation on propeller blades, see Fig. 5. Experimental observations at SVA Potsdam show that, under particular conditions, cavitation bubbles appear on the downstream half of the suction side, as shown in the sketch in Fig. 5. RANS simulation does not produce such cavitation even when a very fine grid is used (here a grid with 29 million cells for a single blade with periodic conditions in circumferential direction was used). With LES-approach and the same grid, cavitation bubbles do appear in the zone indicated by experimental observations. Because the same grid and the same cavitation model is used in both RANS and LES simulations, the difference is obviously due to the turbulence modeling approach alone.

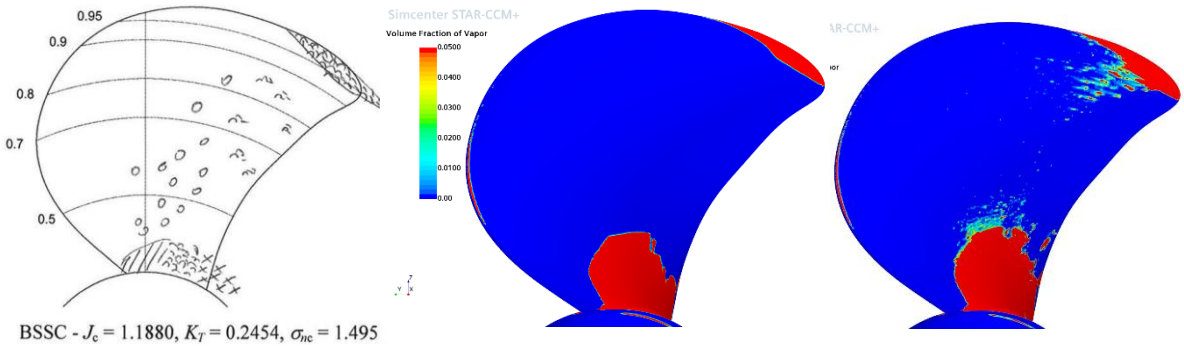

Figure 5 Cavitation on blade suction side: observation in experiment [15] (left), volume fraction of vapor at wall from the RANS solution (middle) and an instantaneous picture from the LES-solution (right).

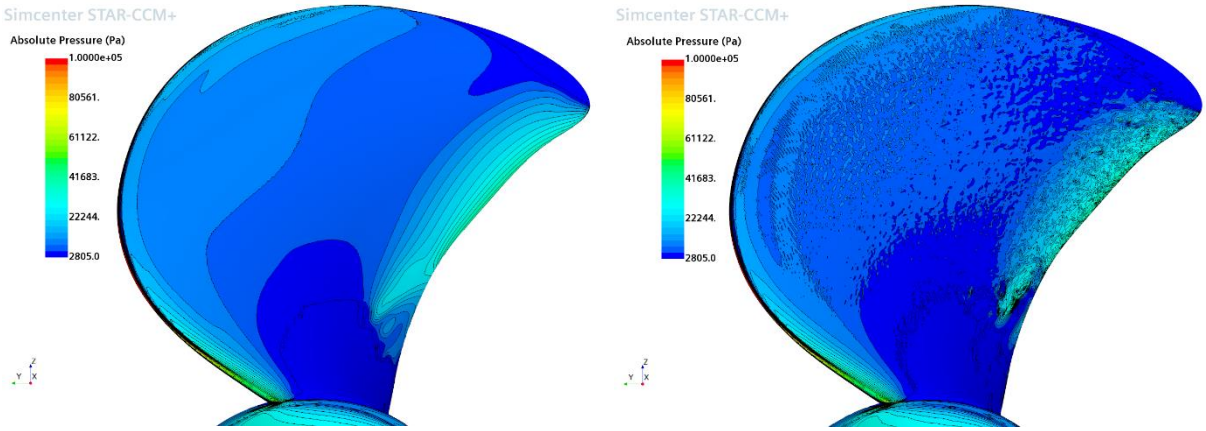

Figure 6 Distribution of instantaneous pressure on the suction side of propeller blade from the RANS-solution (left) and from the LES-solution (right), for the conditions from Fig. 5.

Figure 6 explains why the RANS approach leads to no cavitation on the suction side: the mean pressure resulting from solving the RANS-equations is below the saturation level only in the zones where the tip-vortex cavitation and blade-root cavitation were visible in Fig. 5; over the rest of the suction side of blade surface, the pressure is above saturation level (see Fig. 6 left) and the cavitation does not happen. Even though the RANS-simulation was performed in unsteady mode (here the SST k-ω model was used [6]), the solution was practically steady, except at the edges of the tip-vortex and the blade-root cavitation zones.

In the LES-simulation, turbulent fluctuations of velocity and pressure are resolved up to the grid scale. This is clearly seen in Fig. 6 (right), which shows that pressure not only fluctuates over the blade surface, but that locally low-pressure zones below saturation level are present where the pressure from the RANS simulation is above the saturation level at all times. These small low-pressure zones are created when the fluctuating (fluttering) boundary layer tends to move away from wall. In an animation one can see how the local low-pressure zones appear, move with the flow over some distance and then disappear. The same happens to vapor bubbles: they are created when the pressure falls below saturation level, and they move until the pressure rises again above saturation level, leading to bubble collapse. Therefore, this kind of bubbly cavitation can only be predicted by turbulence modeling approaches which resolve velocity and pressure fluctuations; RANS methods do not fall into this category, because they compute the mean (Reynolds-averaged) quantities. Note that the sketch in Fig. 5 shows experimental observation of local appearance of bubbles during a longer period of time (not everywhere all the time), while the picture from LES shows an instantaneous situation which changes with time.

Figure 7 shows pressure distribution in a longitudinal section through the blade and propeller hub, computed on the same grid using RANS and LES approach to turbulence simulation. The main features are similar, but there are also important differences:

- LES solution shows turbulent fluctuations behind the hub and near the blade wall, where the contours from RANS-simulation are smooth;
- Pressure in the tip vortex core is much lower in the LES than in the RANS-simulation;
- The low-pressure zone on the pressure side near blade root is larger in the LES than in the RANS-solution.

These differences are important under the conditions leading to hub and tip-vortex cavitation.

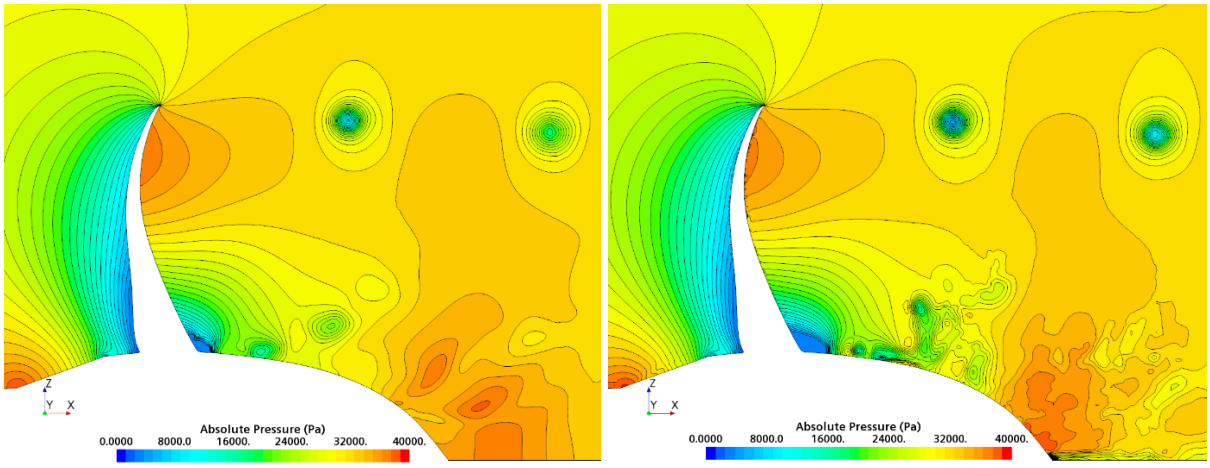

Figure 7 Distribution of instantaneous pressure in the longitudinal section through propeller blade from the RANS solution (left) and from the LES solution (right), for the conditions from Fig. 5.

When studying the flow around a propeller mounted on a vessel, the velocity field approaching propeller is highly inhomogeneous. A propeller blade encounters during its 360° rotation different velocity field (both in magnitude and direction) and different turbulence levels. In order to accurately predict cavitation and especially the hydro-acoustics features, it is important to account for the effects of turbulence in the incoming flow on the flow around propeller blades. In open water or cavitation tunnel tests, the level of turbulence in the flow upstream of propeller is usually very low and uniform, which is not representative of the real application. Unfortunately, applying LES to the flow around the whole hull and all appendages is not possible in practical applications, not even at model scale. However, one could do an embedded LES of the flow around propeller, provided that turbulent fluctuations in the upstream flow are sufficiently accurately reconstructed from the RANS-solution in the whole flow domain. Such simulations are just emerging [16-18] and more applications of this kind are expected in future.

If one is forced to use the RANS approach (as is the case when performing simulations at full scale), it is possible to partially account for the effects of turbulent pressure fluctuations by means of Reynolds stresses, because the fluctuations of velocity and pressure are related [19]. Although there is little data for the validation of such models, they can provide useful information related to cavitation inception.

6. Incipient Cavitation

It is often important to determine under which conditions the cavitation process begins. If cavitation has to be avoided (e.g., in an optimization study in which one of the objectives is to find a design without cavitation), it is often not necessary to perform a two-phase flow analysis with a particular cavitation model. From a single-phase analysis, one can recognize whether cavitation will be taking place or not by examining the pressure distribution in the solution domain. If the pressure locally falls below saturation level, then cavitation will be taking place. However, it may be difficult to determine whether the resulting cavitation is significantly affecting the flow and device performance or not. If the pressure is only slightly below saturation level or if a low pressure is found only within a very small volume, the cavitation effect may be negligible. Criteria to determine the cavitation inception are also not unique in experiments: usually, an engineer observing the flow needs to decide when to classify the flow as being affected by the incipient cavitation.

Figure 8 shows iso-surfaces of saturation pressure (2873 Pa absolute) from a two-phase simulation of flow around the PPTC propeller using the Schnerr-Sauer cavitation model [11] and from a single-phase flow without a cavitation model, compared with iso-surface of 5% vapor volume fraction from the two-phase flow simulation. When the cavitation model is not activated, the zone of low pressure is larger than in the case of a two-phase flow, and also somewhat larger than the zone in which the vapor volume fraction is higher than 5%. Also, in the case of a single-phase flow, the minimum value of absolute pressure is significantly lower than in the case of a two-phase flow: -23,902 Pa compared with 2,732 Pa (141 Pa below saturation pressure), see Fig. 9.

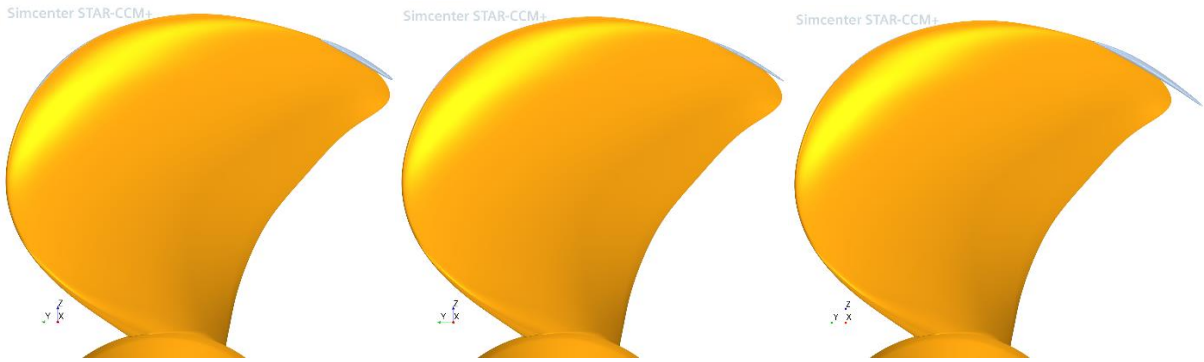

Figure 8 Simulation of incipient cavitation around PPTC propeller: the iso-surface of 5% vapor volume fraction (left) and the iso-surface of saturation pressure (middle) from a two-phase computation using the Schnerr-Sauer cavitation model, and the iso-surface of saturation pressure from a single-phase computation (right).

Table 2 Comparison of solutions from a two-phase and a single-phase simulation of the flow around the PPTC propeller under incipient tip-vortex cavitation conditions with experimental data of SVA Potsdam (Case No. 3, page 2.9) [20]

	Thrust	Torque
Experiment	218.28 N	13.54 Nm
Two-phase simulation	216.50 N (-0.82 %)	13.83 Nm (+2.14 %)
Single-phase simulation	216.05 N (-1.07 %)	13.82 Nm (+2.04 %)

In spite of the differences in details between solutions from single-phase and two-phase simulations of flows with an incipient cavitation, the integral quantities of engineering interest do not differ much, as can be seen from Table 2. The thrust from the single-phase simulation is only 0.25% lower than from the two-phase simulation on the same grid, while the difference in torque is only 0.1%.

In many cases cavitation occurs at more than one location in the flow (e.g., blade leading edge, blade root, tip vortex, hub vortex). When this is the case, one has to use the two-phase simulation to predict the propeller performance, because cavitation does not start at the same time at all locations. The single-phase prediction is only sufficient – with a suitable criterion – to determine the very first occurrence of cavitation.

Note that a negative absolute pressure in the liquid phase may occur even when the cavitation model is active in a two-phase flow simulation. Inside vortexes and recirculation zones, where the residence time of vapor bubbles is long enough, pressure remains close to

saturation level. However, in flow zones where the flow acceleration is very high and the residence time for bubbles is very short (e.g. on the suction side near leading edge), the pressure in liquid my become very low, leading to very high bubble growth rates but not necessarily a high vapor volume fraction. An example is shown in the next section.

7. Tip-Vortex Cavitation

Prediction of tip-vortex cavitation has always been a great challenge. It was long believed that cavitation models used in CFD (like the Schnerr-Sauer model [11] used here) are not capable of predicting this type of cavitation. This view was supported by the fact that the usual grid-dependence studies suggested that no significant changes in the solution would happen with a further refinement, because the thrust and the torque were well converged while tip-vortex cavitation was limited to a small zone near blade tip, see Fig. 9.

The location of tip vortex can be visualized by creating an iso-surface of vorticity, as shown in Fig. 9. By locally refining the grid within the vorticity iso-surface in the tip vortex zone to a sufficiently low level, one can better resolve the extremely high gradients of velocity and pressure across the tip vortex. A section through a such locally refined grid (4.73 million cells in total for a solution domain consisting of a single blade, with periodic conditions in circumferential direction) is shown in Fig. 10. The cell size within the tip vortex core was 0.234 mm (D/1068, where D is the propeller diameter, here 250 mm). The grid is also refined within the hub vortex zone. The flow is from left to right; the setup parameters correspond to Case No. 5 on Page 2.13 in [14]. One finer grid was also created by reducing the cell size everywhere in all directions by a factor of 1.5, leading to a total number of cells around 17 million.

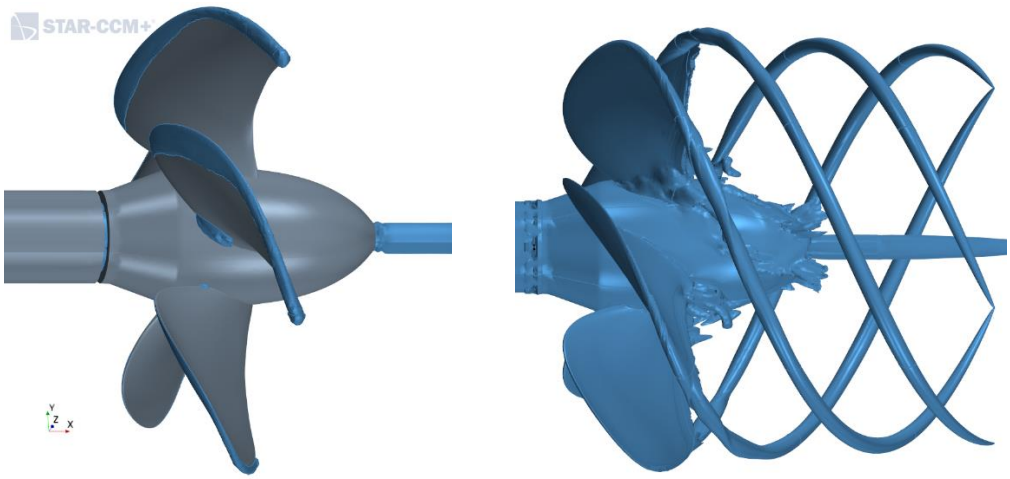

Figure 9 Iso-surfaces of 5% vapor volume fraction (left) and of vorticity magnitude (right), from the computation of a cavitating flow around the PPTC propeller [14] using RANS approach, a version of the k-ε turbulence model [21], the Schnerr-Sauer cavitation model [11], and a grid without local refinement in the vortex core.

Another simulation using a locally refined grid within the vortex core and the RANS approach with a version of the k-ε turbulence model [21] and the Schnerr-Sauer cavitation model [11] shows an improvement compared to the result obtained without a local grid refinement, cf. Figs. 9 and 11. However, the improvement is moderate even when the finest grid with 17 million cells for a single blade is used, as shown in Fig. 11: the tip-vortex cavitation ends too soon, even though the grid was refined to a much longer distance

downstream of propeller. The thrust is relatively well predicted – 1.8 % smaller than in experiment. However, the thrust was almost equally well predicted already on the grid without a local refinement, where practically no cavitation in the tip-vortex was obtained.

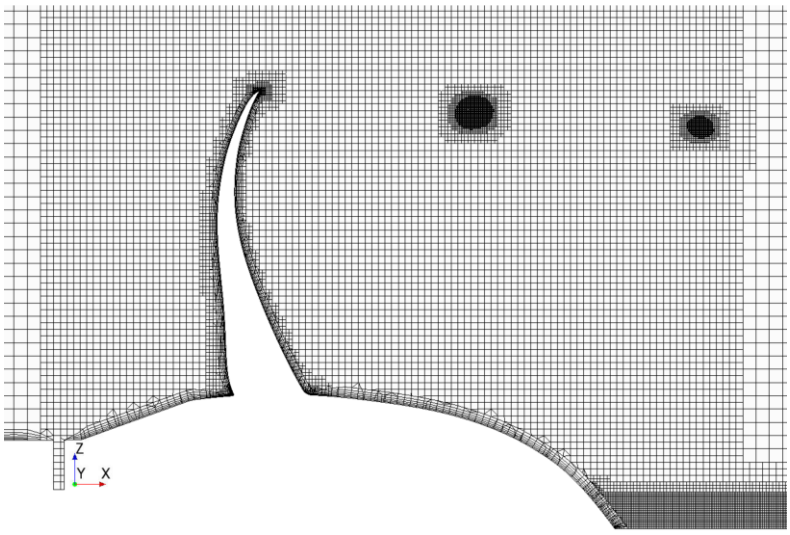

Figure 10 A longitudinal section through the computational grid, showing thelocal refinement within the tip vortex zone, as indicated by the vorticity iso-surface from Fig. 9.

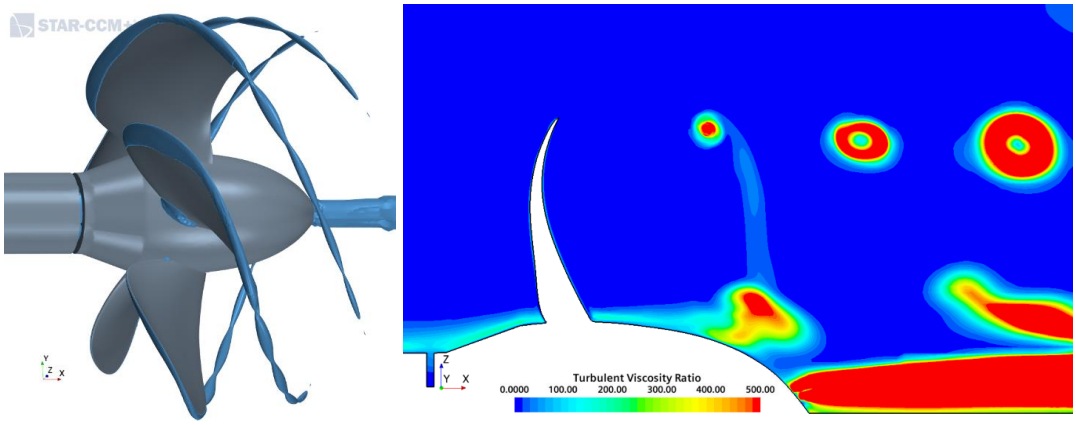

Figure 11 Iso-surfaces of 5% vapor volume fraction (left) and the contours of turbulent viscosity ratio (right) from a RANS computation of the flow around the PPTC propeller [14] using a locally refined grid with 17 million cells for a single blade.

The finest grid is so fine, that even the LES-approach to turbulence modeling can be used. The WALE model was applied to account for the unresolved part of turbulence [8], but the grid near wall was not fine enough to fully resolve the viscous sublayer of the boundary layer on propeller blades, so wall functions were use. However, the focus here was to capture the tip-vortex cavitation, and for this the wall treatment is not essential.

As can be seen from Fig. 12, with the LES approach to modeling the effects of turbulence, tip-vortex cavitation is very well captured: the picture of iso-surface of the vapor volume fraction 0.05 looks very similar to the photograph of tip-vortex cavitation taken in the experiment [14]. This shows that the turbulence model plays a more important role for the prediction of tip-vortex cavitation than the cavitation model; the simple Schnerr-Sauer model [11] produces a pretty good solution when applied together with LES. The thrust obtained from LES-simulation is ca. 3.8 % too high; this is most probably due to the insufficiently fine grid near walls. The DES approach (Detached-Eddy Simulation) uses the RANS approach near walls, for which the current grid was adequate, and the LES in zones away from wall. This sounds like a good choice for the flow around propeller blade. Indeed, the results

obtained with IDDES (Improved Delayed DES, [22]) produces the best solution: the tip-vortex cavitation extends as far as the grid is fine enough, like in the LES, but the thrust is now 1.5 % below the measured value. The RANS approach produced a similar agreement between simulation and experiment for the thrust and torque – but with an insufficient level of tip-vortex cavitation, cf. Figs. 11 and 13. The question is now: why is the turbulence model so important for capturing the tip-vortex cavitation? The answer comes from the comparison of turbulent viscosity ratios (the ratio of turbulent viscosity over fluid viscosity) from RANS and DES simulations presented in Figs. 11 and 13. While in DES and LES simulations the level of turbulent viscosity in the tip vortex zone is very low, every RANS model produces there a significantly higher turbulent viscosity. This high turbulent viscosity leads to smearing of velocity gradients, and that in turn leads to an increase in pressure. Once the pressure in the tip-vortex zone becomes higher than the saturation level, the cavitation stops.

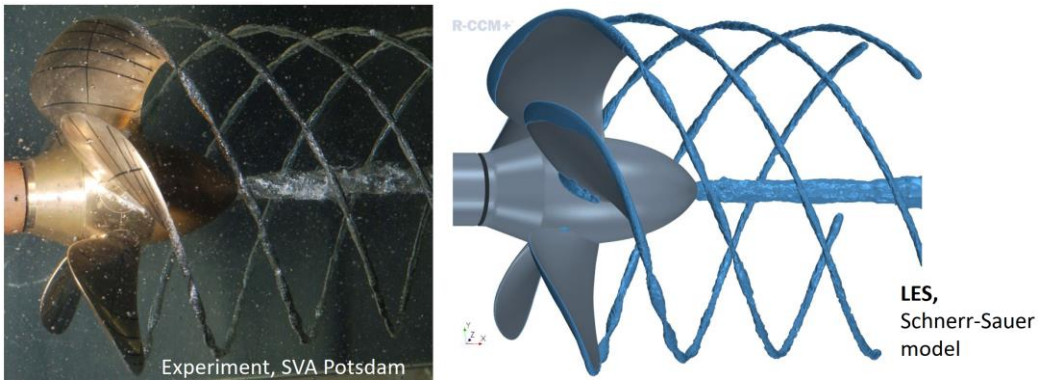

Figure 12 A photograph of tip-vortex cavitation pattern in the experiment (left [14]) and iso-surfaces of 5% vapor volume fraction (right) from an LES-computation of flow around the PPTC propeller [14] using the finest grid with 17 million cells for a single blade.

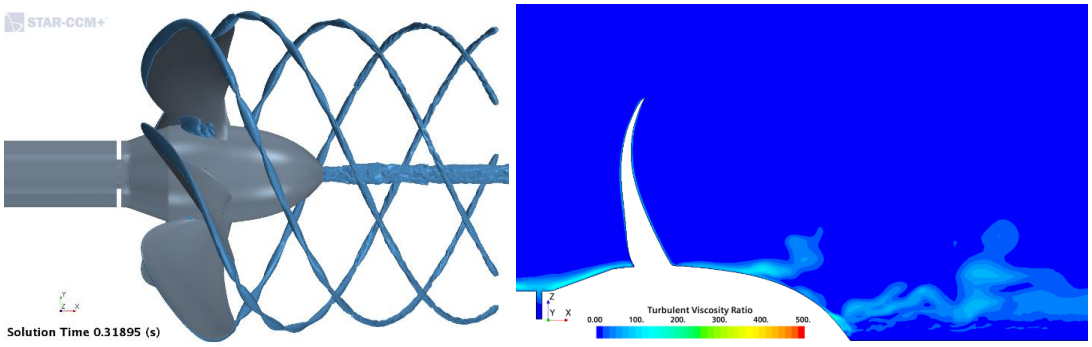

Figure 13 Iso-surfaces of 5% vapor volume fraction (left) and contours of turbulent viscosity ratio (right) from a DES-computation of flow around the PPTC propeller [14] using the finest grid with 17 million cells for a single blade.

The pressure inside the tip vortex cavitation zone is nearly constant and only slightly below the saturation level, as can be seen from Fig. 14. However, outside the vortex core the pressure increases very rapidly, as can be seen from dense pressure contours around the vortex core and from the profile across vortex core shown in Fig. 15. The streamwise velocity component is also almost constant inside the vortex core, as shown in Fig. 15, but the gradients with which the velocity decreases on one side and increases on the other side of the vortex core are extremely high. Thus, for a successful prediction of tip-vortex cavitation one needs a fine grid to resolve the extreme pressure and velocity gradients around the tip vortex core, and a turbulence model which does not generate too high turbulent viscosity in this

zone, in spite of high velocity gradients. Taking into account that the cavitation model used [11] is based on relatively crude approximations (as discussed in Sect. 2) and that the results are quite satisfactory when the grid is fine enough and an appropriate turbulence model is sued, one can conclude that for tip-vortex cavitation prediction the grid fineness and the turbulence model are more important than the cavitation model.

Figure 14 also shows that in a small zone within hub vortex and close to the blade tip, the absolute pressure is below -1000 Pa (the minimum pressure at the suction side near leading edge is actually much lower). As discussed in Sect. 6, this is physically correct because (i) pure liquids can sustain tensile stresses (i.e., a negative pressure) to a relatively high degree, and (ii) the bubble growth rate is finite. Thus, where fluid velocity is very high and the residence times of bubbles within the low-pressure zone are short, the absolute pressure in liquid can be negative. Inside cavitation bubbles (which are not resolved in the kind of cavitation models used here) and in zones with a very high vapor volume fraction, the absolute pressure must, of course, be positive because the gas phase cannot support tensile stresses. Within sheet, hub vortex and tip vortex cavitation, the pressure is close to the saturation level, as shown in Fig. 15.

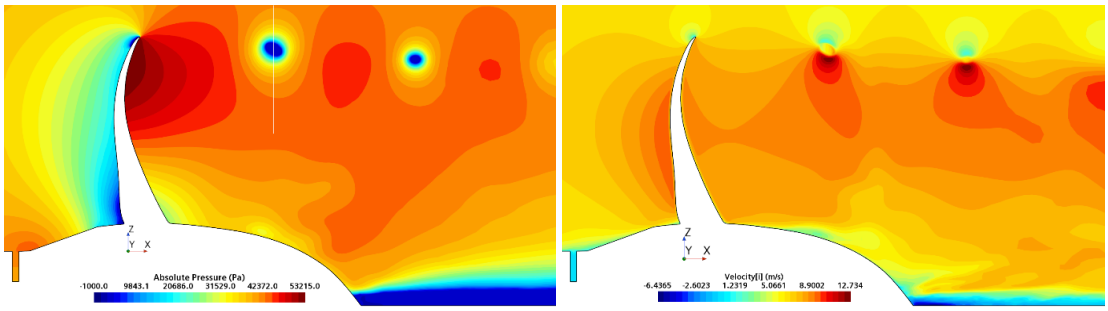

Figure 14 Contours of the absolute pressure (left) and the axial velocity component (right) in a longitudinal section through the blade and hub, from a DES-computation of flow around the PPTC propeller [14] using a locally refined grid with 4.73 million cells for a single blade (the while line in the left figure indicates where profiles from Fig. 15 are taken).

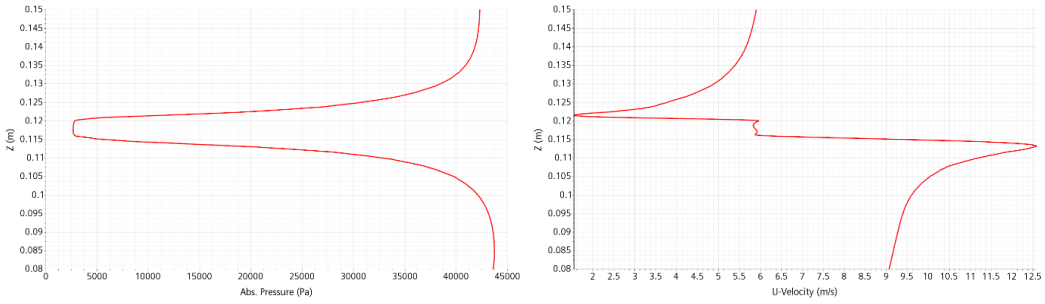

Figure 15 Profiles of absolute pressure (left) and axial velocity component (right) along a vertical line through the center of tip vortex downstream of propeller blade (as indicated by a while line in Fig. 14), from a DES-computation of flow around propeller using locally refined grid with 4.73 million cells for a single blade.

8. Scale Effects

Scale effects play an important role in ship hydrodynamics: it is practically impossible to match both Froude and Reynolds numbers in an experiment at model scale and in full scale. The same is true for studies of cavitating flows around propeller: the model-scale propeller used in experiments is ca. 40 times smaller than the full-scale propeller, and it

rotates much faster. For this reason, cavitation is present on each propeller blade during its full rotation in model scale, while at full scale, cavitation is present only during ca. 1/3rd of the rotation, see Fig. 16. The pressure increases by 1 bar from top to bottom of the propeller in full scale (for a propeller with a diameter of 10 m), while the variation is very small in model scale. As Fig. 16 shows, the similarity between the cavitation pattern in model and full scale is limited, making an extrapolation of results obtained in model scale to the full scale application rather difficult.

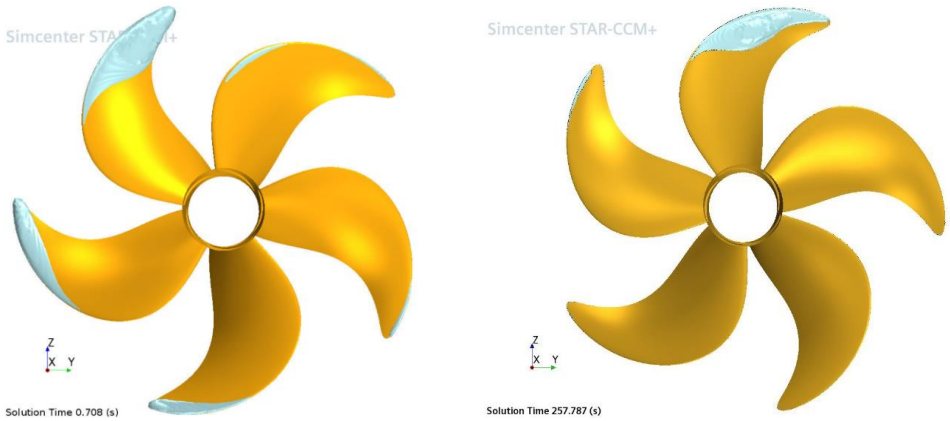

Figure 16 Iso-surfaces of 5% vapor volume fraction on propeller blades: model scale (left) and full scale (right).

Another problem with cavitation studies in model scale is that the experiment is usually performed in a cavitation tunnel of a relatively small cross-section and without free surface, i.e. the boundary conditions in laboratory and in full-scale operation are not even similar. Thus, the flow around propeller is different from what it would be if the free surface was present and the blockage effects were negligible. The reflection of pressure waves from the walls of cavitation tunnel is also problematic, especially if pressure fluctuations on propeller blades, rudder and hull above propeller are studied. Experiments are trusted as representing the "truth", which is true at the model scale – but that truth is not the one the engineers need to know! Besides, the measurement data is also affected by uncertainties. It is not unusual that the results from experiments performed in different cavitation tunnels for the nominally the same flow differ by as much as the difference between simulation and experiment.

Performing a flow simulation at full scale is hardly any more difficult than at model scale: one only needs to reduce the relative thickness of the near-wall cells compared to the grid that would be suitable for a simulation at model scale, in order to ensure that the same number of cells is present within the logarithmic range of the boundary layer. Another important aspect of a full-scale simulation is that the natural conditions for the flow can be realized (a free surface with waves instead of the cavitation tunnel top wall; an infinite environment instead of the high blockage of the tunnel cross-section and the tunnel walls which reflect pressure waves; etc.). The problem of different time scales for the build-up of ship-induced waves and the cavitation on propeller blades can be overcome by using a two-stage simulation process. In the first stage, the cavitation is deactivated and the time step is selected as appropriate for the computation of ship resistance (order of 100 time steps per time period needed for the fluid to travel one ship length). One can even replace the propeller at this stage by a virtual disc model, i.e. use appropriate momentum source terms instead of a physical propeller. Once the resistance and the wave pattern have stabilized, the second stage begins with an activated cavitation model and a rotating propeller, using time steps appropriate for the cavitation analysis (order of 100 time steps per blade-passing period).

The problem is that full-scale data is scarce and the confidence in full-scale simulation is therefore still limited. Although the quality of CFD predictions has been verified in

numerous comparisons between simulation and experimental data, the suspicion is still large, even though nothing is suggesting that the accuracy of CFD solutions could be lower at full than at model scale. As more data from full-scale measurements becomes available (hopefully in near future), the confidence in full-scale simulations will increase.

9. Conclusions

In this paper some important aspects and challenges in simulations of cavitating flows, especially of flows around propellers, were examined. A CFD simulation of a cavitating flow can be accurate – sometimes even more accurate than a model-scale experiment – but it is important to understand the potential sources of errors, their relative effect on the results, and how to reduce them as much as possible. Cavitation on propellers can be predicted with a satisfactory accuracy using common cavitation models (like the Schnerr-Sauer model [11]), provided that the grid is locally refined within appropriate zones (around the leading edge, within the tip vortex, within the hub vortex etc.). Capturing the tip-vortex cavitation requires also a turbulence model which does not produce excessive turbulent viscosity. LES and DES types of models are appropriate, but there are also proposals to avoid excessive turbulent viscosity in RANS-model, like the so-called Reboud-correction [23]. An accurate representation of propeller geometry by the computational grid is also important. Especially the insufficient resolution of the leading-edge curvature can falsify the geometry and affect the splitting of the flow to the pressure and suction sides of propeller blades and cause premature flow separation or cavitation. Simulation can be used to study the effects of manufacturing tolerances (shape of the blades and the deviation of built geometry compared to the CAD model). In ship hydrodynamics, one of the most important tasks is to determine the hull resistance and to choose an appropriate propeller whose thrust matches the resistance at a minimum of required power. The workshop organized by Lloyds Register in 2016 demonstrated that full-scale simulation of self-propulsion can be reliably conducted with state-of-the-art CFD-software [24]. With the scaling effects undermining the accuracy of extrapolations from model tests, and with an increasing body of evidence that CFD simulations at full scale are achieving the engineering-level accuracy, the move to simulating full-scale propeller performance under actual operating conditions will become state-of-the-art method for designing efficient and reliable ships.

REFERENCES

[1] *Cavitation in control valves*. Technical Information, Samson AG, www.samson.de.

[2] Ferziger, J.H., Perić, M., Street, R.L., 2018. *Computational Methods for Fluid Dynamics*, Springer Nature, Cham, Switzerland.

[3] Durbin, P. A., & Pettersson Reif, B. A., 2011. *Statistical theory and modeling for turbulent flows* (2nd ed.). Chichester, England: Wiley. https://doi.org/10.1002/9780470972076

[4] Pope, S. B., 2000. *Turbulent flows*. Cambridge: Cambridge Univ. Press.

[5] Wilcox, D. C., 2006. *Turbulence modeling for CFD* (3rd ed.). La Cañada, CA: DCW Industries, Inc.

[6] Menter, F. R., 1994. Two-equation eddy-viscosity turbulence models for engineering applications. *AIAA J.*, **32**, 1598-1605. https://doi.org/10.2514/3.12149

[7] Smagorinsky, J., 1963. General circulation experiments with the primitive equations. Part I: The basic experiment. *Monthly Weather Rev.*, 91, 99-164. https://doi.org/10.1175/1520-0493(1963)091<0099:GCEWTP>2.3.CO;2

[8] Nicoud, F., Ducros, F., 1999. Subgrid-scale stress modelling based on the square of the velocity gradient tensor. *Flow, Turbulence and Combustion*, 62, 183-200. https://doi.org/10.1023/A:1009995426001

[9] Symposia on Marine Propulsors, permanent site: https://www.marinepropulsors.com/ accessed 25th July 2022.

[10] Muzaferija, S., Papoulias, D., Perić, M., 2017. VOF simulations of hydrodynamic cavitation using the asymptotic and classical Rayleigh-Plesset models. In *Proc. 5th Int. Symp. On Marine Propulsion smp'17*. Espoo, Finland, June 2017.

[11] Schnerr, G. H., Sauer, J., 2001. Physical and numerical modeling of unsteady cavitation dynamics. In *Fourth international conference on multiphase flow*. New Orleans, USA.

[12] https://www.sva-potsdam.de/wp-content/uploads/2020/11/PPTC-update_on_cavitation-VP1304vsP1790-1-1.pdf accessed 25th July 2022.

[13] Jin, S., Zha, R., Peng, H., Qiu, W., Gospodnetic, S., 2020. 2D CFD studies on effects of leading-edge propeller manufacturing defects on cavitation performance. SNAME Maritime Convention 2020 – A Virtual Event, Sept. 29th - Oct. 2nd, 2020.

[14] SVA Report No. 3753, page 2.13, Case No. 5 (https://www.sva-potsdam.de/wp-content/uploads/2016/03/SVA-report-3753.pdf) accessed 25th July 2022.

[15] SVA Report No. 3753, page 2.9, Case No. 40 and page 3.15 (https://www.sva-potsdam.de/wp-content/uploads/2016/03/SVA-report-3753.pdf) accessed 25th July 2022.

[16] Deck, S., 2012. Recent improvements in the Zonal Detached Eddy Simulation (ZDES) formulation. *Theor. Comput. Fluid Dyn.* 26, 523–550. https://doi.org/10.1007/s00162-011-0240-z

[17] De Laage de Meux, B., Audebert, B., Manceau, R., Perrin, R., 2015. Anisotropic linear forcing for synthetic turbulence generation in large eddy simulation and hybrid RANS/LES modeling. *Physics of Fluids*, 27 (3), 035115. https://doi.org/10.1063/1.4916019

[18] Skillen, A., Revell, A., Craft, T., 2016. Accuracy and efficiency improvements in synthetic eddy methods. *International Journal of Heat and Fluid Flow*, 62, 386-394. https://doi.org/10.1016/j.ijheatfluidflow.2016.09.008

[19] Ferziger, J. H., 1983. Higher level simulations of turbulent flow," in *Computational Methods for Turbulent, Transonic, and Viscous Flows* (J.-A. Essers, ed.), Hemisphere, Washington D.C, USA.

[20] SVA Report No. 3753, page 2.9, Case No. 3 (https://www.sva-potsdam.de/wp-content/uploads/2016/03/SVA-report-3753.pdf) accessed 25th July 2022.

[21] Lardeau, S., 2018. Consistent strain/stress lag eddy-viscosity model for hybrid RANS/LES. In Y. Hoarau, S. H. Peng, D. Schwamborn, & A. Revell (Eds.), *Progress in Hybrid RANS-LES Modelling* (p. 39-51). Springer, Cham, Switzerland. https://doi.org/10.1007/978-3-319-70031-1_4

[22] Spalart, P.R., Deck, S., Shur, M.L., Squires, K.D., Strelets. M., Travin, A., 2006. A new version of detached eddy simulation, resistant to ambiguous grid densities. *Theoretical Computational Fluid Dynamics*, 20, 181-195. https://doi.org/10.1007/s00162-006-0015-0

[23] Reboud, J.L., Stutz, B., Goutier, O., 1998. Two-phase flow structure of cavitation: experiment and modeling of unsteady effects. In *Proc. Third Int. Symp. on Cavitation.* Grenoble, France, Apr. 7th-10th.

[24] D. Ponkratov (Ed.), Proceedings: 2016 Workshop on Ship Scale Hydrodynamic Computer Simulations, Lloyd's Register, Southampton, United Kingdom (2017).

Submitted: 31.05.2022.
Accepted: 25.07.2022.

Milovan Perić
University of Duisburg-Essen,
CoMeT Continuum Mechanics Technologies GmbH
milovan@comet-cfd.de